Analytical solution of the depth-averaged flow velocity in case of submerged rigid cylindrical vegetation

Fredrik Huthoff,[1,2] Denie C. M. Augustijn,[1] and Suzanne J. M. H. Hulscher[1]

Received 17 November 2006; revised 15 February 2007; accepted 12 March 2007; published 16 June 2007.

[1] A new model for the depth-averaged velocity for flow in presence of submerged vegetation is developed. The model is based on a two-layer approach, where flow above and through the vegetation layer is described separately. Vegetation is treated as a homogeneous field of identical cylindrical stems, and the flow field is considered stationary and uniform. It is demonstrated that scaling considerations of the bulk flow field can be used to avoid complications associated with smaller scale flow processes and that still the behavior of depth-averaged flow over vegetation is described accurately. The derived scaling expression of the average flow field is simple in form, it follows fundamental laws of fluid flow, and it shows very good agreement with laboratory flume experiments. The new model can be used for quick evaluation of a river's hydraulic response in cases where vegetated floodplains are inundated.

Citation: Huthoff, F., D. C. M. Augustijn, and S. J. M. H. Hulscher (2007), Analytical solution of the depth-averaged flow velocity in case of submerged rigid cylindrical vegetation, *Water Resour. Res.*, *43*, W06413, doi:10.1029/2006WR005625.

1. Introduction

[2] The presence of vegetation in floodplains may have significant influence on the overall discharge capacity of a river [e.g., *Darby*, 1999]. In particular, if floodplains are relatively wide compared to the main channel, realistic predictions of stage-discharge relations rely strongly on accurate knowledge of floodplain flow. Therefore it is crucial to understand the processes that contribute to floodplain resistance and the hydraulic impacts these processes may have.

[3] The interplay between walls or solid objects and the flow field causes vortices and swirling motions at various length scales. Trying to represent these detailed flow characteristics is an immense task, which even with the most modern equipment is impossible for spatial and temporal scales that are relevant in river engineering studies. Consequently, depth-averaged quantities and scaling considerations are often used to arrive at bulk flow descriptions. Several such relations exist that relate the average flow velocity to surface characteristics, for example, by means of a roughness height [*Strickler*, 1923; *Nikuradse*, 1933; *Keulegan*, 1938]. However, if the irregularities or resistance elements are of the same order of magnitude as the flow depth, available methods to predict flow resistance are no longer valid [e.g., *Smart et al.*, 2002; *Stone and Shen*, 2002]. If, for example, a flow field is penetrated by vegetation, turbulent vortices are created in the wakes downstream of the protruding stems [e.g., *Akilli and Rockwell*, 2002]. The associated energy losses of the mean flow field cause the flow to slow down. These drag effects can even become more important than energy losses because of friction at the channel bed [e.g., *James et al.*, 2004]. Therefore conventional resistance equations (based on wall roughness) are no longer appropriate when describing flow through vegetation. In such cases, both bed resistance and drag effects have to be taken into account in order to arrive at a representation of hydraulic resistance that covers a wide range of conditions realistically.

[4] Several previous investigations have focused on effects of vegetative resistance in river flows. Experimental campaigns have been set up to measure flow resistance in natural vegetated fields [see, e.g., *Green*, 2006]. Experiments in laboratory flumes have been carried out, with some recent studies by *Stephan and Gutknecht* [2002], *Järvelä* [2002], *Wilson et al.* [2003], and *Armanini et al.* [2005]. Also, detailed numerical simulations of flow through vegetation were performed [e.g. *Shimizu and Tsujimoto*, 1994; *Erduran and Kutija*, 2003; *Neary*, 2003; *Choi and Kang*, 2004]. As a result of such studies, several relations were proposed that describe flow resistance caused by vegetation. Some of these relations are empirical [*Ree and Crow*, 1977; *Kouwen and Fathi-Moghadam*, 2000], others have stronger theoretical foundations [*Petryk and Bosmajian*, 1975; *Stone and Shen*, 2002]. Also, there are methods that are based on modified logarithmic-velocity profiles [e.g., *Kouwen and Unny*, 1973; *Stephan and Gutknecht*, 2002], which are a well-established experimental characteristic of turbulent wall-bounded flows and find theoretical justification in similarity arguments [e.g., *Schlichting*, 1979]. *Klopstra et al.* [1997] combined methodologies by treating flow over vegetation in a two-layer approach, where the flow in two layers is described separately. They combined a modified logarithmic velocity profile in the surface layer with a newly derived velocity profile that is present in between the vegetation.

[5] Among the existing vegetation-resistance relations, the empirical ones have the advantage of being simple in form. On the other hand, empirical relations have the

[1]Department of Water Engineering and Management, University of Twente, Enschede, Netherlands.
[2]HKV Consultants, Lelystad, Netherlands.

0043-1397/07/2006WR005625$09.00

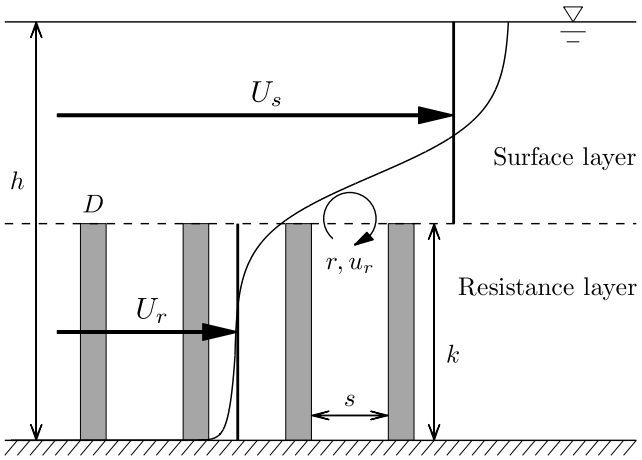

Figure 1. In the two-layer approach for flow with submerged vegetation, the height of the vegetation k marks the interface between the resistance layer and the surface layer (h is the total flow depth). The average velocity in the resistance layer U_r is determined by a balance between the streamwise component of the gravitational force, bed resistance, form drag, and shear stress due to flow over the vegetation (section veglayer). Flow in the surface layer (U_s) is described with an equivalent bed roughness model.

drawback that their applicability is limited to the range of conditions for which they were derived. Theoretical descriptions often are complex. Besides, they may require poorly understood closure parameters and sometimes pose practical difficulties when gathering required input data.

[6] In the current work, a new scaling expression of the average flow field is proposed that combines advantages of existing flow equations, (1) it is simple in form, (2) it is based on fundamental (flow) principles, (3) it depends on readily measurable quantities and, most importantly, shows excellent agreement with experimental data. The method is based on a two-layer approach, similar as done by *Klopstra et al.* [1997], where flow in and above the vegetation is treated separately. However, here we only consider bulk characteristics of the flow field by which we avoid difficulties associated with depth-averaging of flow velocities. Vegetation is replaced by cylindrical stems that are homogeneously distributed and have identical geometrical and material properties. Furthermore, the vegetated channel is considered to be sufficiently wide, such that sidewall effects can be neglected. An improved understanding of processes in these idealized conditions will eventually lead to a better description of flow through natural vegetation.

[7] In section 2, the concept of the two-layer approach is explained. Next, in sections 3 and 4, the proposed velocity descriptions for the two flow layers are derived. A comparison with selected data from flume experiments is made in section 5, which subsequently yields the new calibrated model for the depth-averaged velocity of flow with submerged vegetation.

2. The Two-Layer Approach

[8] In a flow field over a solid boundary, the force balance between gravitation and flow resistance leads to an equilibrium flow state, which can be associated with a characteristic average flow velocity. For steady uniform flow, this condition is expressed as

$$\rho g h i = \rho f U^2 \tag{1}$$

where the streamwise component of the gravitational force (per unit length and width) depends on the density of water ρ, the gravitational acceleration g, the depth of flow h, and the channel slope i. Dimensional analysis requires that for a dimensionless bed-friction function f, the average flow velocity enters the bed resistance term as U^2. For flow over a solid boundary, several formulations for f have been proposed to reflect energy losses due to wall friction (see the work of *Yen* [2002] for an overview). *Strickler* [1923] proposed a power law dependence on the relative roughness height k_S / h, where k_S reflects the height of irregularities at the bed:

$$f_S = \frac{1}{64}\left(\frac{k_S}{h}\right)^{1/3}. \tag{2}$$

A theoretical justification for equation (2) is given by *Gioia and Bombardelli* [2002], who have shown that the given power law dependence is valid for turbulent flow over a hydraulically rough bed. This condition is usually met in natural rivers.

[9] However, in the situation of flow over vegetation, not only the bed friction slows down the flow but also the drag caused by the vegetation. Therefore an additional resistance term τ_v is added to the force balance from equation (1), which results in [e.g., *Petryk and Bosmajian*, 1975; *Wu et al.*, 1999; *Stone and Shen*, 2002]

$$\rho g h i = \rho f U^2 + \tau_v. \tag{3}$$

Equation (3) describes the force balance in a flow layer that is penetrated by vegetation.

[10] If the vegetation is submerged in a flow field, then flow above the vegetation is not directly obstructed by the individual plants. The flow in this particular layer experiences resistance because of a slower flowing region in between the vegetation. The resistance to flow in the surface layer can therefore be described by an equivalent bed shear stress. Hence the depth-averaged velocity in this surface layer is determined by a force balance equivalent to equation (1).

[11] In summary, assuming that all vegetation has the same height, for overflown vegetation two distinct flow layers can be distinguished that have different characteristic flow velocities (see Figure 1):

[12] 1. The flow layer that is penetrated by the vegetation (i.e., the "resistance layer") with average velocity U_r and

[13] 2. The flow layer above the vegetation (i.e., the "surface layer") with average velocity U_s.

[14] The average flow velocity of the entire flow depth (U_T) is found by proportionally adding the average flow velocities of the resistance layer U_r and the surface layer U_s:

$$U_T = \frac{k}{h} U_r + \frac{h-k}{h} U_s, \tag{4}$$

where the height of the vegetation k only partly penetrates the total depth of flow h.

3. The Resistance Layer

3.1. Emergent Vegetation

[15] To derive the average flow velocity in the resistance layer, we first consider the situation where the vegetation is not completely overflown. By replacing the vegetation with a homogeneous field of identical cylindrical stems, the additional resistance τ_v in equation (3) can be replaced by a standard drag force term ("stem drag," [e.g., *Schlichting*, 1979]) to yield:

$$\rho ghi = \rho f {U_{r0}}^2 + \frac{1}{2}\rho C_D m D h U_{r0}^2. \quad (5)$$

[16] The average velocity for flow through emergent vegetation is now denoted by U_{r0}. Individual stems have a diameter D (m), a bed surface density m (m^{-2}), and are characterized by a dimensionless drag coefficient C_D. The separation between neighboring stems follows from $s = 1/\sqrt{m} - D$ (that is, s is measured edge-to-edge). Since U_{r0} is a depth-averaged value, parameters m, s, D, and C_D should be treated accordingly.

[17] The force balance in equation (5) can easily be extended to also take the solidity of the vegetation into account, that is, a factor is introduced that corrects for the surface area and volume occupied by the vegetation [e.g., *Kaiser*, 1984; *Stone and Shen*, 2002; *James et al.*, 2004]. However, *James et al.* [2004] found that such a solidity correction can usually be neglected. The correction on flow velocities and water levels is proportional to D^2 / s^2 [*Huthoff and Augustijn*, 2006]. Therefore only when the stem diameter of the vegetation is of the same order of magnitude as the separation between individual plants, then equation (5) yields significant loss in accuracy.

[18] The product $C_D m D$ in equation (5) carries the dimension (1/m). For further simplification, we therefore introduce a new length parameter (the "drag length")

$$b = \frac{1}{C_D m D}. \quad (6)$$

The drag length b represents the downstream distance over which the mean flow momentum is dissipated because of cylinder drag. On the basis of equation (5), and using the definition for the drag length from equation (6), the average velocity for flow through emergent vegetation U_{r0} is written as [see also *Petryk and Bosmajian*, 1975]

$$U_{r0} = \sqrt{\frac{2bgi}{1 + \frac{2b}{h}f}}, \quad \text{for } h \le k. \quad (7)$$

The average flow velocity U_{r0} can now be determined if the bed resistance function f is known, for example, by using Strickler's relation as given by equation (2).

3.2. Submerged Vegetation

[19] When the cylindrical elements become submerged, the flow in the surface layer will have a higher average velocity as in this layer no drag due to the stems is experienced. The energy losses in the surface layer will be entirely due to a shear stress near the top of the resistance layer, which balances the streamwise component of the gravitational force that drives the flow. The shear stress between the surface layer and the resistance layer (i.e., the "interface shear" τ_k, at height k) will also cause the flow in the resistance layer to speed up. If we introduce the extra shear stress component τ_k due to flow in the surface layer, and realize that the height of the resistance layer is now given by k, the force balance from equation (5) modifies to

$$\tau_k + \rho gki = \rho f {U_r}^2 + \frac{1}{2}\rho C_D m D k {U_r}^2. \quad (8)$$

The velocity in the resistance layer for submerged vegetation is now denoted by U_r. Also, we have assumed that the drag coefficient for an emergent stem is identical to that of a submerged stem, which is reasonable unless the cylinders have small aspect ratios k / D, see [*Sumner et al.*, 2004] who finds distinctly different wake structures if $k / D < 5$.

[20] The shear stress at the top of the resistance layer τ_k balances the gravitational force that acts on the water volume in the surface layer, given as

$$\tau_k = \rho g(h - k)i. \quad (9)$$

Inserting equation (9) into equation (8) yields the force balance for flow in a submerged resistance layer:

$$\rho ghi = \rho f {U_r}^2 + \frac{1}{2}\rho C_D m D k {U_r}^2. \quad (10)$$

The contribution on the left-hand-side of equation (10) is due to the gravitational force that acts both on the surface and the resistance layer. The drag force now acts over a depth k, as opposed to the total flow depth h in the force balance that describes flow through emergent vegetation [equation (5)]. Rearranging terms in equation (10) gives a new description for the average velocity in the resistance layer for submerged conditions:

$$\frac{U_r}{U_{r0}} = \sqrt{\frac{h}{k}}, \quad \text{for } h \ge k. \quad (11)$$

A similar relation to equation (11) has been proposed by *Bentham and Britter* [2003], where the average velocity in the resistance layer is proportional to $\sqrt{h}$. Also, *Smart et al.* [2002] point out that with increasing relative roughness, a conceptual drag coefficient model would lead to a square-root law of the flow resistance.

[21] The average velocity in the resistance layer U_r logically reduces to U_{r0} if no free flowing layer above the cylindrical stems is present (i.e., if $h = k$). After inserting Strickler's bed resistance function f_S as given in equation (2) into equation (10), the scaling velocity U_{r0} is written as:

$$U_{r0} = \sqrt{\frac{2bgi}{1 + \frac{b}{32k}\left(\frac{k_S}{h}\right)^{1/3}}}, \quad \text{for } h \ge k. \quad (12)$$

[22] Considering that the roughness height k_S is usually much smaller than the flow depth h, the contribution of bed

resistance is often negligible. From equation (12), it follows that the average velocity in the resistance layer U_{r0} is practically equal to

$$U_{r0} \approx \sqrt{2bgi}, \quad \text{if } k_S << h. \tag{13}$$

The average flow velocity in the resistance layer can be estimated from equation (13) if there is no information available about the properties of the channel bed. Such an estimate is reasonable for dense or tall emergent vegetation in relatively deep flows (small drag length b, and large vegetation height k and flow depth h). For sparse vegetation distributions (large drag lengths), bed resistance may become the dominant source of flow resistance. This effect is also included in equation (11), which for extremely large drag length b ultimately transforms to Manning's well-known relation for flow over a rough bed.

4. The Surface Layer

4.1. Shear Stress in the Surface Layer

[23] In steady flow over a rough bed, the shear stress at the bed surface balances the gravitational force on the water body. Similarly, for flow over vegetation, resistance to flow in the surface layer is due to a shear stress that originates at the top of the resistance layer. An expression for this shear stress is already given in equation (9). From the Reynolds Averaged Navier-Stokes equation, it follows that the (Reynolds) shear stress at any location in the flow is determined by the magnitude of fluctuations in the velocity field [e.g., *Pope*, 2000]

$$\tau_{xz} = \rho\overline{v_x v_z} \tag{14}$$

where v_x and v_z denote turbulent velocity fluctuations in streamwise and vertical direction (i.e., over depth), respectively.

[24] In the theoretical derivation of Manning's law for rough channel flow, *Gioia and Bombardelli* [2002] assume that streamwise velocity fluctuations v_x scale with the average flow velocity U_s, and that vertical fluctuations v_z are determined by eddies between the roughness elements. It is assumed that a characteristic spatial scale r and characteristic velocity u_r can be associated with these eddies. Following *Gioia and Bombardelli* [2002], the interface shear stress at the artificial bed (i.e., near the top of the resistance layer, see Figure 1) scales as

$$\tau_k \sim \rho U_s u_r. \tag{15}$$

Together with the expression for the interface shear stress as given in equation (9) this yields

$$\rho g(h-k)i \sim \rho U_s u_r. \tag{16}$$

To find a relation for the average velocity in the surface layer U_s, an independent expression for u_r needs to be found. For that purpose, a methodology similar to the one demonstrated by *Gioia and Bombardelli* [2002] is used, which is based on the condition of a constant turbulent energy dissipation rate from large to smaller flow scales (Kolmogorov scaling).

4.2. Turbulent Energy and Kolmogorov Scaling

[25] In the Kolmogorov view on turbulent flow, turbulent energy is created through external forcing at the largest scale of the system (energy containing range) and is dissipated to successively smaller scales until eventually viscosity damps the smallest flow patterns [e.g., *Pope*, 2000]. The rate of production of turbulent kinetic energy per unit mass is denoted by ε (m^2/s^3) and, at large scales, is independent from the viscosity (Kolmogorov's second similarity hypothesis). For the energy input at the largest scale, a scaling expression for ε is obtained that is composed of representative geometrical parameters and the representative flow velocity. For surface layer flow as depicted in Figure 1, it seems natural to choose the depth of the surface layer ($h - k$) for the geometrical spatial parameter and the average surface velocity U_s for the representative velocity. Dimensional analysis yields

$$\varepsilon \sim \frac{U_s^3}{h-k}. \tag{17}$$

Furthermore, the concept of an energy cascade, in which turbulent energy is transferred from large to smaller spatial scales, requires that energy dissipated at small spatial scales equals production at the largest scale of the system [e.g., *Pope*, 2000]. In our particular case, if it is assumed that eddies of size r and velocity u_r dominate the flow field near the artificial rough bed (i.e., at the top of the vegetation), the dissipation rate scales as

$$\varepsilon \sim \frac{u_r^3}{r}. \tag{18}$$

Now ε is related to the characteristic velocity u_r and a length scale r, which represents the extent of local eddies. The characteristic velocity in the resistance layer can be related to the average velocity in the surface layer as [using equations (17) and (18)]

$$u_r \sim U_s\left(\frac{r}{h-k}\right)^{1/3}. \tag{19}$$

The scaling relation for flow in the surface layer, equation (19), is only valid if there is no length scale between scales $h - k$ and r where significant additional sources of turbulent energy occur that affect the energy cascade (i.e., existence of a spectral gap, e.g., *Pouquet et al.* [1983], *Nikora et al.* [1997]). For flows over vegetation, convincing evidence has been found for enhanced turbulent energy production at length scales associated with wake dimensions [e.g., *Raupach et al.*, 1986; *Nezu and Onitsuka*, 2001; *Naden et al.*, 2006]. However, these features seem to be most pronounced at depths well into the resistance layer [e.g., *Poggi et al.*, 2004] and thus do not have severe implications for the assumptions leading to equation (19).

[26] Next, equation (19) is inserted into equation (16), which yields a scaling expression for the average velocity in the surface layer:

$$U_s \sim \left(\frac{h-k}{r}\right)^{1/6}\sqrt{g(h-k)i}. \tag{20}$$

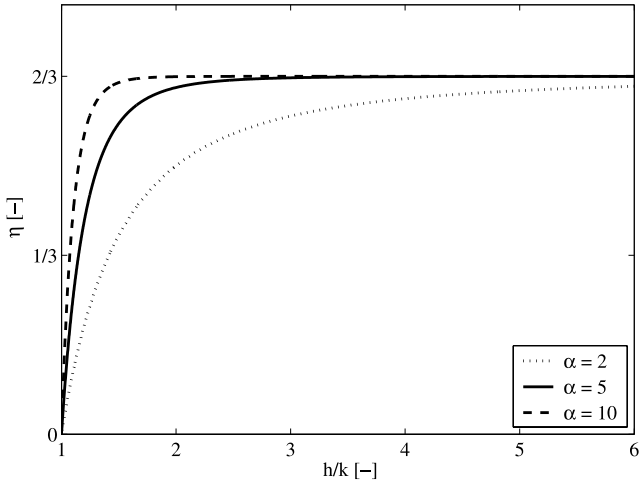

Figure 2. Possible functions of the exponent η in equation (23), when assuming incomplete similarity between the dimensionless flow velocity in the surface layer (U_s / U_{r0}) and the depth of the surface layer $h - k$. Larger values for α result in faster transitions from $\eta = 0$ to $\eta = 2/3$ [see equation (24)].

Note that equation (20) reduces to the Manning/Strickler equation [*Manning*, 1889; *Strickler*, 1923] if the spacing hydraulic radius r is independent of flow depth. It is well-established that for turbulent flow over rough-walls, the relation between the average flow velocity and wall-characteristics is represented by Manning's formula [*Chow*, 1959; *Silberman et al.*, 1963; *Yen*, 2002]. This will be used as a limiting condition, in case the depth of the surface layer becomes much larger than the roughness elements.

4.3. Similarity Considerations

[27] The velocity in the surface layer can be treated as a dimensionless quantity by scaling U_s to the characteristic velocity in the resistance layer U_{r0}. The same scaling methodology was followed to arrive at equation (11) for the dimensionless velocity in the resistance layer. Assuming that the dimensionless velocity in the surface layer shows similarity with respect to the surface layer depth ($h - k$), the following power law asymptotic is defined:

$$\frac{U_s}{U_{r0}} \sim \left(\frac{h-k}{\ell}\right)^{\eta}. \tag{21}$$

An unknown scaling length ℓ is introduced in equation (21), which is determined from comparison with experimental data (section 5).

[28] If in equation (20) r indeed reflects an equivalent roughness height, at large depths, the power law exponent in equation (21) must have the value $\eta = 2/3$:

$$\frac{U_s}{U_{r0}} \sim \left(\frac{h-k}{\ell}\right)^{2/3}, \quad \text{for } h >> k. \tag{22}$$

However, a property of equation (22) is that U_s reduces to 0 when the surface layer vanishes (i.e., when h approaches k). This behavior is not realistic because the average flow velocity in the surface layer should always be larger than the flow velocity in the resistance layer (U_{r0}), even if the surface layer is extremely shallow. Essentially, the power law in equation (22) does not give realistic results when the depth of the surface layer, $h - k$, becomes close to or smaller than the scaling length ℓ. This can be solved if we assume incomplete similarity in the surface layer depth $h - k$, and no kind of similarity in the relative depth h / k (see the work of *Barenblatt* [2003] for theory on complete and incomplete similarity). Assuming incomplete similarity in $h - k$, we allow the power exponent η in equation (21) to be variable (depending on the relative flow depth h / k):

$$\frac{U_s}{U_{r0}} \sim \left(\frac{h-k}{\ell}\right)^{\eta(h/k)}. \tag{23}$$

We have already argued that for large depths, the power exponent η should approach 2/3, in correspondence with Manning's resistance law. However, as h approaches k, the velocity in the surface layer U_s should approach U_{r0}, which requires that η vanishes. In summary:

$$(i) \text{ if } h/k >> 1 \text{ then } \eta \rightarrow 2/3,$$

$$(ii) \text{ if } h/k \rightarrow 1 \text{ then } \eta \rightarrow 0.$$

[29] These conditions are met when η is defined as

$$\eta = \frac{2}{3}\left(1 - \left(\frac{h}{k}\right)^{-\alpha}\right), \quad \text{for } \alpha > 0. \tag{24}$$

Equation (24) describes the transition from a power exponent $\eta = 2/3$ to $\eta = 0$ as the depth of the surface layer decreases (i.e., as h approaches k). The exponent α determines how quickly η makes this transition (Figure 2).

[30] Inserting equation (24) into the scaling equation for the average velocity in the surface layer, equation (23), yields

$$\frac{U_s}{U_{r0}} \sim \left(\frac{h-k}{\ell}\right)^{\frac{2}{3}\left(1-\left(\frac{h}{k}\right)^{-\alpha}\right)}. \tag{25}$$

Thus, we have derived a new model for the average velocity in the surface layer. For large flow depths, equation (25) transforms to Manning's law. For shallow surface layer flows, it approaches the drag-dominated velocity in the resistance layer.

5. Comparison to Data From Flume Experiments

5.1. Flume Experiments

[31] For model calibration, we use the experimental data from the work of *Meijer and van Velzen* [1998] (for data, see also the work of *Baptist* [2005]). The available experimental data comprise 48 flow experiments with homogeneously distributed cylindrical stems that all have the same stem diameter (D = 8 mm). The cylinder height k varied between three distinct values (k = 0.45, 0.9, or 1.5 m), and flow depths h were varied such that relative depths were in the range from $h / k = 1.3$ to $h / k = 5.5$. Half of the total set of experiments was carried out with a surface density m of 256 cylindrical stems per square meter (s = 5.5 cm), the other half with a surface density of $m = 64$ m^{-2} (s = 11.7 cm).

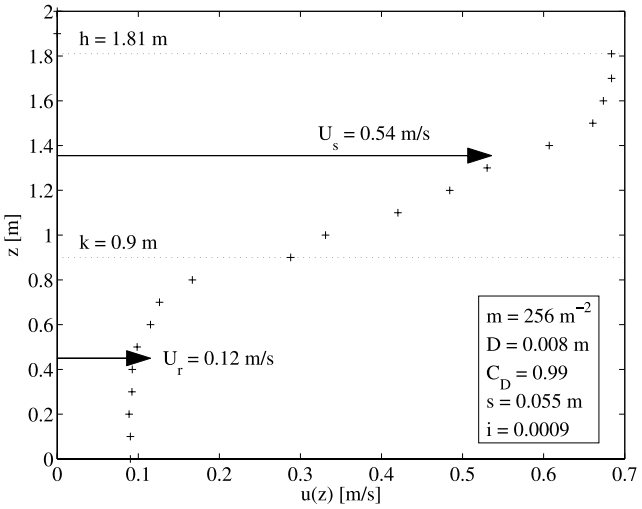

Figure 3. Measured velocity profile (+) for 1 of the 48 flow experiments with rigid cylindrical vegetation [*Meijer and van Velzen*, 1998]. Arrows depict the magnitude of the depth-averaged velocities in the surface layer U_s and the resistance layer U_r.

[32] For each of the experiments, flow velocities were measured at depths 0.10 m apart with an Acoustic Doppler Velocimeter. Using linear interpolation, the average flow velocity for the surface layer U_s and the resistance layer U_r were estimated separately (see Figure 3). The characteristic velocity U_{r0} was determined by depth-averaging the flow velocity in the lower part of the resistance layer, which was unaffected by the flow in the surface layer.

[33] On the basis of four flow experiments without artificial vegetation, the roughness height k_S of the flume bed was determined $k_S = 2.3 \pm 0.6$ mm. Also, from eight experiments with emergent cylinders, drag coefficients were determined from measured flow velocities and measured surface slopes (using equation 5). The resulting drag coefficients were compared with values predicted for flow around isolated cylinders. For this purpose, local Reynolds numbers were calculated from the measured average velocities in the resistance layer ($Re \sim 3 \times 10^4$–4×10^4) and subsequently, the drag coefficients C_D for the circular cylinders. Standard works on fluid mechanics [e.g., *Schlichting*, 1979] report that in such a flow regime, the drag coefficient remains fairly constant with a value of nearly 1. Measured C_D values were quite evenly spread around predicted values, and it was concluded that the observed deviation from the predicted drag coefficients was largely due to measurement errors in the surface slope [*Meijer*, 1998]. No significant variations in the drag coefficient were observed that could be attributed to sheltering effects for objects placed in an array [e.g., *Raupach*, 1992; *Nepf*, 1999]. Consequently, for the remaining 48 experiments with submerged cylinders, predicted C_D values were adopted and surface slopes were corrected to match the measured characteristic velocity U_{r0} in the lower resistance layer.

5.2. Average Velocities in the Two Flow Layers

[34] Figure 4 shows the measured average velocities in the resistance layer as compared with the ones predicted by equation (11). Although for slow flows the velocities are slightly overestimated, the overall agreement between equation (11) and measured values is very good ($R^2 = 0.94$).

[35] The scaling expression for the velocity in the surface layer, equation (25), consists of two unknown parameters, the scaling length ℓ and the transition exponent α. Table 1 shows some model results using different geometrical quantities for the scaling length ℓ and the corresponding values for α that fit the measurements best (maximum R^2). It turns out that for $\ell = Ks$, the proposed scaling law gives best agreement with laboratory data. This particular scaling approach is not very sensitive to changes in α, as any α value in the range 4–7 still yields a coefficient of determination larger than 0.97 if compared with laboratory data. The maximum of R^2 occurs when α is very close to 5 ($R^2 = 0.98$), with a corresponding coefficient of proportionality K practically equal to unity. Therefore we propose the following expression for the scaling length ℓ in the surface layer:

$$\ell = s. \tag{26}$$

In combination with a value for the transition exponent of $\alpha = 5$ in equation (24), the new scaling relation for the flow velocity in the surface layer becomes

$$\frac{U_s}{U_{r0}} = \left(\frac{h-k}{s}\right)^{\frac{2}{3}\left(1-\left(\frac{h}{k}\right)^{-5}\right)}. \tag{27}$$

[36] Figure 5 shows how the predictions of the calibrated scaling expression, equation (27), compare to the measured flow velocities. Surface layer velocities are predicted accurately for the entire data set of 48 experiments.

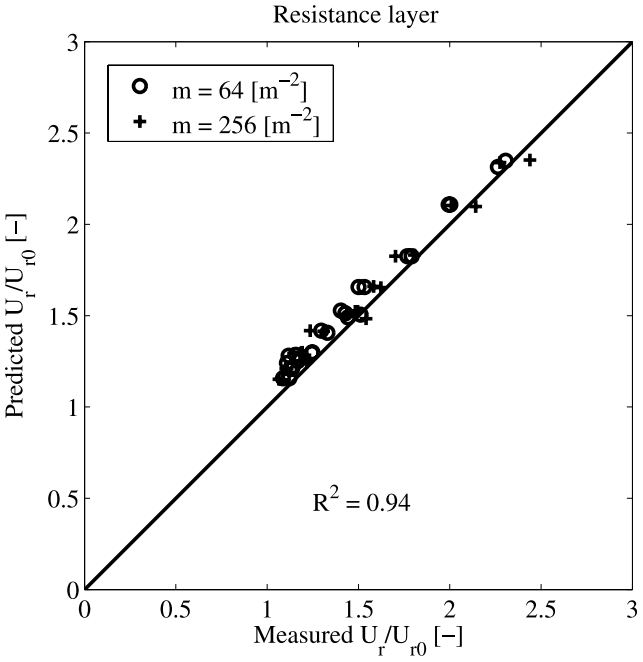

Figure 4. Comparison between the proposed model for the depth-averaged velocity U_r in the resistance layer [equation (11), on vertical axis] and results from laboratory flume experiments (m = number of cylindrical stems per m^{-2} on the bed surface).

Table 1. Model Results to Predict the Average Velocity in the Surface Layer Using Equation (25)[a]

ℓ	K	α	R^2	99% Conf. Int
Ks	0.87	3	0.94	(0.88–0.97)
Ks	0.95	4	0.975	(0.95–0.99)
Ks	0.99	5	0.981	(0.96–0.99)
Ks	1.00	6	0.977	(0.95–0.99)
Ks	1.00	7	0.97	(0.93–0.98)
Kb	0.093	4	0.85	(0.70–0.93)
KD	9.5	5	0.60	(0.33–0.79)
KC_DD	9.8	5	0.59	(0.31–0.78)
Kk	0.13	50	0.33	(0.07–0.60)

[a]For different geometric quantities to describe the scaling length ℓ, the optimal value for exponent α is determined (in case $\ell = Ks$ five values for α are shown).

[37] As shown in section 4.2, theory predicts a depth-independent scaling length ℓ, and a constant power of 2/3, when the depth of the surface layer is large. By comparison with experimental data (with relative depths in the range $h / k = 1.3–5.5$), we found that shallow flows are also well described by introducing a transition exponent of $\alpha = 5$ in equation (24). This value for α implies that the exponent η only deviates significantly from 2/3 for relative flow depths $h / k < 2.5$ (see Figure 2). Therefore even though the scaling relation given in equation (22) was only expected to give realistic results for deep surface layer flows, it also performs well for flows in relatively shallow surface layers when using the scaling length $\ell = s$ [equation (26)]. If we would assume complete similarity between flow velocity and depth of the surface layer [i.e., by using a constant exponent $\eta = 2/3$ in equation (25)], small values of U_s / U_{r0} are predicted less accurately, but still a coefficient of determination of $R^2 = 0.94$ is found.

5.3. A Two-Layer Scaling Model for the Entire Flow Depth

[38] By using the newly proposed flow velocity models for the resistance layer [equation (11)] and the surface layer [equation (27)], the expression for the average velocity of the entire flow depth [equation (4)] becomes:

$$\frac{U_T}{U_{r0}} = \sqrt{\frac{k}{h}} + \frac{h-k}{h}\left(\frac{h-k}{s}\right)^{\frac{2}{5}\left(1-\left(\frac{k}{h}\right)^{-5}\right)} \tag{28}$$

[39] In Figure 6, the predictions of the new two-layer velocity scaling model for the entire flow depth [equation (28)] are compared with the measured average flow velocities. The combined performance of the velocity models in the resistance and surface layer [equations (11) and (27)] is even better than their separate predictions, yielding a coefficient of determination $R^2 = 0.99$.

[40] In section 5.2, it was addressed that the variable power exponent η in the surface layer only affects predicted flow velocities for relatively shallow surface layers (if $h / k < 2.5$). For the average velocity over the entire depth [equation (28)], this effect is even further suppressed because for shallow surface layers, the overall flow field is largely determined by flow in the resistance layer. Therefore predictions of depth-averaged flow velocities are not very sensitive to the choice of parameter α in equation (25).

6. Discussion

6.1. Length Scales in the Surface Layer

[41] The scaling length ℓ, reflecting the flow resistance that the surface layer experiences because of the cylindrical elements, is well represented by the spacing between the

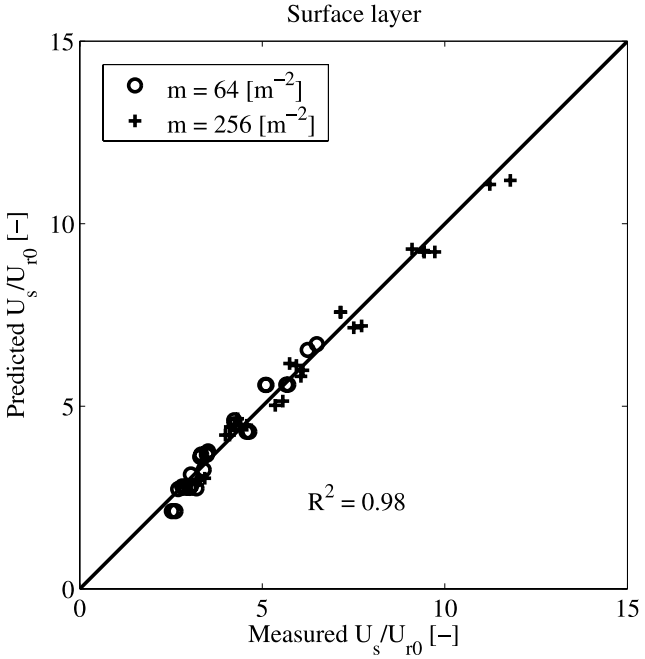

Figure 5. Measured and predicted values [equation (27)] of the depth-averaged velocity U_s in the surface layer.

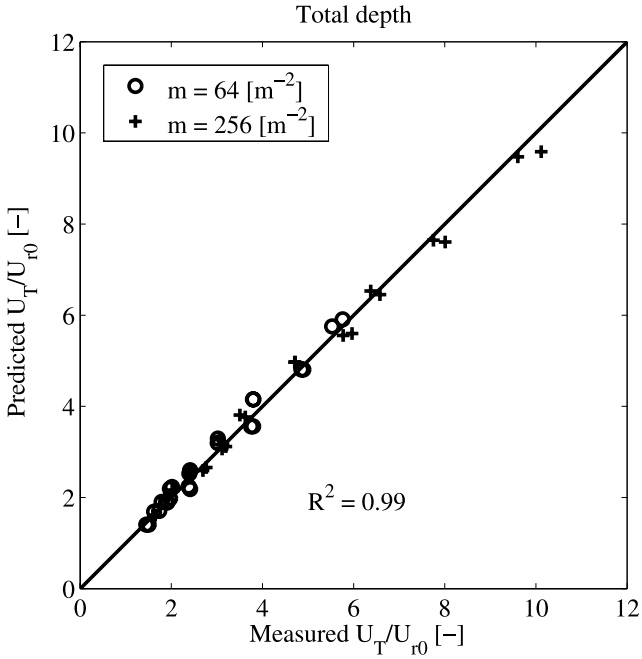

Figure 6. The predicted depth-averaged velocity over the entire flow depth [U_T as in equation (28), on vertical axis] versus measured average velocities.

cylindrical stems s. This may seem a surprising result since earlier studies have shown that the shear length scale at the interface between surface and resistance layer [defined as $L = U(\partial U/\partial z)^{-1}$ at $z = k$] reflects the turbulent length scale that is responsible for most vertical momentum transfer [e.g., *Raupach et al.*, 1996; *Ghisalberti and Nepf*, 2004]. While correlations between L and k (the vegetation height) sometimes yield good results [*Raupach et al.*, 1996], in general, a scaling relation $L \sim k$ cannot be correct. This conclusion is supported by observations of flow over tall resistance elements with only limited extent of the shear layer [e.g., *Ghisalberti and Nepf*, 2004]. Also in Figure 3, a limited shear layer is shown; in the lower half of the resistance layer, the velocity profile is practically vertical. In the region of vertical velocity profile, neither bed effects nor surface layer effects significantly influence the flow field. Thus, energy losses are due to cylinder drag. Departure from a vertical velocity profile in the upper half of the resistance layer is due to flow in the surface layer but is entirely detached from bed roughness effects. Therefore if bed effects have negligible influence on the mean flow in the resistance layer, the shape of the velocity profile at the top of the cylinders is not controlled by the distance to the bed.

[42] If a general scaling length exists for flow over tall objects, then it can only be related to scales that are present at the top of the resistance layer, such as the stem diameter, or the spacing between neighboring elements. Both *Raupach et al.* [1996] and *Ghisalberti and Nepf* [2004] acknowledge that the interface shear, or conversely, the shear scaling length L, is related to vegetation density. In view of these observations, the drag length b, which depends on vegetation density and reflects momentum dissipation because of cylinder drag, appears to be a suitable candidate for a turbulent length scale. Furthermore, Table 1 shows that $\ell = b$ also yields good results when compared with laboratory data ($R^2 = 0.85$). Here we reflect on some implications associated with choosing $\ell = b$ instead of $\ell = s$.

[43] First of all, it is important to note that the scaling length ℓ is merely introduced to make equation (21) dimensionally correct, as it seems natural to scale the flow velocity in the surface layer to the characteristic velocity U_{r0} in the resistance layer. The turbulent length scale r in equation (20) reflects the equivalent size of eddies responsible for the momentum transfer in the resistance layer. Combining equations (13), (20), and (22) reveals that both length scales are related as

$$r \sim \frac{\ell^4}{b^3} \tag{29}$$

Next, we consider the drag length b and the spacing between cylinders s as possible values for the scaling length ℓ:

1. If $\ell = b$ then $r \sim b$.

2. If $\ell = s$ then $r \sim s^4/b^3$.

[44] The drag length b can be expressed as

$$b = \frac{(s+D)^2}{C_D D} \tag{30}$$

(see equation 6), which yields for the turbulent length scales:

1. If $\ell = b$ then $r \sim (s+D)^2/(C_D D)$.

2. If $\ell = s$ then $r \sim (C_D D)^3/(s+D)^2$.

[45] Assuming that the turbulent scale r reflects the equivalent length scale where most momentum transfer takes place [an equivalent 'roughness height', see equation (20)], then a larger r is associated with larger resistance to flow. In terms of cylinder geometry and distribution, larger resistance is associated with increasing diameter D and decreasing separation s. This behavior is found in option 2, while option 1 gives the opposite behavior (if $s > D$). Therefore it is concluded that the drag length b cannot be a suitable value for the scaling length ℓ.

[46] Having discarded b as suitable scaling length for ℓ, the alternative $\ell = s$ remains a likely candidate. The analysis above has shown that $\ell = s$ is associated with a turbulent length scale r that increases with increasing stem diameter and vegetation density. Such general trends are indeed expected, but the exact form of the scaling function for r is not well understood.

[47] Also, interpreting the turbulent scale r as an equivalent roughness height (for surface layer flow), it seems natural to assume that r may not exceed the height of the cylinders k. Subsequently, ℓ should always be smaller than $(kb^3)^{1/4}$ for $\ell = s$ to be valid. Further investigations with different geometrical properties of the cylinders, and different spatial distributions, should be carried out to study these situations.

6.2. Hydraulic Resistance of Natural Vegetation

[48] Complications arise when we want to represent hydraulic resistance of natural vegetation with the newly proposed two-layer flow model. In the proposed flow model, the plant height k is considered fixed and identical for all individual plants. A fixed value for the plant height k allowed us to define two distinct flow layers. Is this still possible when the plant height is spatially variable, or when in case of flexible vegetation bending effects decrease the depth of the resistance layer? An average plant height is possibly still appropriate for defining two flow layers if plant height variability is concentrated around a well-pronounced mean value. If, however, the distribution of different heights shows distinct peaks, then more flow layers should be defined, each associated with an average flow velocity. Plant flexibility not only changes the effective height of the vegetation but may also alter the effective drag force because of streamlining. *Järvelä* [2004] has proposed a solution to this problem by introducing the vegetation parameter χ, which serves as a correction factor on the drag force.

[49] Also, the spacing parameter s, which reflects the spatial density of the vegetation, is easily determined for a homogeneous field of identical stems. However, which value should be used for a representative plant separation if the spatial distribution of individual plants is not homogeneous, or when variability between plants exists and side branches with leaves also obstruct the flow? For flow through emergent vegetation, this problem is more easily

Table 2. Effective Geometrical Parameters of Selected Floodplain Vegetation Types [*van Velzen et al.*, 2003][a]

Vegetation Type	m^2	D	s	k	s / D	k / D
Natural Grassland	4000–5000	0.003	0.011–0.013	0.1–0.2	4	33–67
Sedges	200	0.006	0.065	0.3	11	50
Thistle Bushes	1000–3000	0.003	0.015–0.029	0.3	5–10	100
Bramble Bushes	112	0.005	0.089	0.5	18	100
Pipe Grass	300	0.004	0.054	0.5	13	125
Reed-Mace	20	0.018	0.21	1.5	11	83
Reed	80	0.005	0.11	2.5	22	500
Orchards	0.16	0.1–0.2	2.3–2.4	2–3	11–24	15–20
Softwood Shrub	3.8	0.034	0.48	6	14	176
Dense Cylinders	256	0.008	0.055	0.45–1.5	6.9	45–188
Sparse Cylinders	64	0.008	0.117	0.45–1.5	14.6	45–188

[a]Also listed are geometrical parameters of the cylindrical stems used in the current study.

solved because the drag coefficient C_D can be adjusted to match flow measurements for a specific choice of plant separation (or similarly, a choice of frontal plant area, see, for example, the work of *Fischenich and Dudley* [2000]). Whether it is justified to use this same plant separation value to determine the flow velocity in the surface layer when the vegetation becomes overflown is questionable. Relating to this issue, *Järvelä* [2004] proposed a method to estimate an effective diameter for branched vegetation. Along the same lines, it would be interesting to investigate whether an effective plant separation allows for application of the new model to real vegetation. *van Velzen et al.* [2003] gives a list of effective surface densities and stem diameters for a range of typical floodplain vegetation types. Comparing the effective ratios k/D and s/D for natural vegetation with the ranges investigated in the present study shows that the proposed hydraulic resistance model potentially covers a wide range of vegetation types, including grasses, reed, sedges, and several types of bushes (Table 2).

7. Conclusions

[50] In the present study, flow over large-scale roughness elements is described by an average-velocity model where distinct flow characteristics are attributed to two separate flow layers. By describing flow by its bulk behavior, we avoided the necessity of integration over depth and the associated complications of depth-dependent turbulence intensities. Predictions of the new expression for the depth-averaged velocity for flow with submerged rigid vegetation gives excellent agreement with measured flow velocities (coefficient of determination $R^2 = 0.99$).

[51] The new proposed models that describe the depth-averaged flow velocity in the two flow layers separately also each show very good agreement with measured flow velocities. It was shown that depth-averaged flow in the resistance layer is adequately described by means of a simple bulk-force balance. Apart from the drag coefficient that is particular to the shape of the resistance elements, no further calibration parameter is needed for the resistance layer model. For the surface layer, a comparison with results from flume experiments shows that the scaling length ℓ, required in the depth-averaged velocity relation, is well represented by the spacing between the cylindrical stems. A depth-dependent power law exponent is used to force the scaling law to a realistic limiting value for relatively shallow surface layer flows. This adaptive power exponent improves predicted velocities in the surface layer if the vegetation penetrates about half of the total water column, until vegetation becomes emergent (and the surface layer vanishes). For relatively larger depths of the surface layer, average flow velocities follow Manning's resistance law.

[52] The proposed flow resistance model is based on idealized vegetation characteristics with homogeneous geometrical and material properties. Because of its accurate predictions for such conditions, it may serve as a reliable basis for describing the hydraulic response to natural vegetation.

Notation

b Drag length
C_D Drag coefficient
D Diameter of cylindrical resistance elements
f Bed resistance function
f_S Strickler's bed resistance function
g Gravitational acceleration
h Flow depth
i Energy slope
k Height of resistance elements
k_S Strickler's roughness height
K Coefficient of proportionality
ℓ Scaling length
L Shear length scale (in mixing layer)
m Bed surface density of resistance elements
r Turbulent length scale (roughness height)
s Separation between individual resistance elements
R^2 Coefficient of determination
u_r Characteristic eddy-velocity near top of resistance elements
U_{r0} Depth-averaged flow velocity in the resistance layer for emergent resistance elements
U_r Depth-averaged flow velocity in the resistance layer
U_s Depth-averaged flow velocity in the surface layer
U_T Depth-averaged flow velocity over total flow depth
$v_{x,z}$ Velocity fluctuations in streamwise and vertical direction, respectively
α Transition exponent
ε Energy dissipation rate
η Similarity exponent
ρ Water density
τ_k Shear stress at top of resistance layer
τ_v Vegetation drag

[53] **Acknowledgments.** This research is supported by the Technology Foundation STW, applied science division of NWO, and the technology program of the Ministry of Economic Affairs (Netherlands).

References

Akilli, H., and D. Rockwell (2002), Vortex formation from a cylinder in shallow water, *Phys. Fluids*, *14*(9), 2957–2967.

Armanini, A., M. Righetti, and P. Grisenti (2005), Direct measurement of vegetation resistance in prototype scale, *J. Hydraulic Res.*, *43*(5), 481–487.

Baptist, M. J. (2005), Modelling floodplain biogeomorphology, Ph.D. thesis, Delft University of Technology.

Barenblatt, G. I. (2003), Scaling, *Cambridge Texts in Applied Mathematics*, Cambridge Univ. Press, New York.

Bentham, T., and R. Britter (2003), Spatially averaged flow within obstacle arrays, *Atmos. Environ.*, *37*, 2037–2043.

Choi, S. U., and H. Kang (2004), Reynolds stress modeling of vegetated open-channel flows, *J. Hydraulic Res.*, *42*(1), 3–11.

Chow, V. T. (1959), *Open-channel Hydraulics*, international edition 1973 ed., McGraw-Hill, New York.

Darby, S. (1999), Effect of riparian vegetation on flow resistance and flood potential, *J. Hydraulic Eng.*, *125*(5), 443–454.

Erduran, K. S., and V. Kutija (2003), Quasi-three-dimensional numerical model for flow through flexible, rigid, submerged and non-submerged vegetation, *J. Hydroinformatics*, *5*(3), 189–202.

Fischenich, C., and S. Dudley (2000), Determining drag coefficients and area for vegetation, *Ecosytem Management & Restoration Research Program SR 08*, US Army Corps of Engineers.

Ghisalberti, M., and H. Nepf (2004), The limited growth of vegetated shear-layers, *Water Resour. Res.*, *40*, W07502, doi:10.1029/2003WR002776.

Gioia, G., and F. A. Bombardelli (2002), Scaling and similarity in rough channel flows, *Phys. Rev. Lett.*, *88*(1), 14,501–14,504.

Green, J. C. (2006), Effect of macrophyte spatial variability on channel resistance, *Adv. Water Res.*, *29*, 426–438.

Huthoff, F., and D. C. M. Augustijn (2006), Hydraulic resistance of vegetation: Predictions of average flow velocities based on a rigid-cylinders analogy, *Civil Engineering & Management report 2006R-001/WEM-003 (ISSN 1568-4652)*, University of Twente.

James, C. S., L. Birkhead, and A. A. Jordanova (2004), Flow resistance of emergent vegetation, *J. Hydraulic Res.*, *42*(4), 390–398.

Järvelä, J. (2002), Flow resistance of flexible and stiff vegetation: A flume study with natural plants, *J. Hydrol.*, *269*, 44–54.

Järvelä, J. (2004), Determination of flow resistance caused by non-submerged woody vegetation, *J. River Basin Manage.*, *2*(1), 61–70.

Kaiser, W. (1984), Fliesswiderstandsverhalten in Gerinnen mit Ufergebüsch, *Wasserbau-Mitteilungen Heft 23*, TH Darmstadt.

Keulegan, G. H. (1938), Laws of turbulent flow in open channels, *J. Res. Natl. Bur. Stand.*, *21*(Research paper 1151).

Klopstra, D., H. J. Barneveld, J. M. van Noortwijk, and E. H. van Velzen (1997), Analytical model for hydraulic roughness of submerged vegetation, in *Managing Water: Coping with scarcity and abundance*, pp. 775–780, Proceedings of the 27th IAHR Congress, San Fransisco.

Kouwen, N., and M. Fathi-Moghadam (2000), Friction factors for coniferous trees along rivers, *J. Hydraulic Eng.*, *126*(10), 732–740.

Kouwen, N., and T. E. Unny (1973), Flexible roughness in open channels, *J. Hydraulics Div.*, *HY5*.

Manning, R. (1889), On the flow of water in open channels and pipes, *Trans. Inst. Civil Eng. Ireland*, *20*, 161–207.

Meijer, D. G. (1998), Modelproeven overstroomde vegetatie, *Tech. Rep. PR121*, HKV Consultants, Lelystad, Netherlands.

Meijer, D. G., and E. H. van Velzen (1998), Prototype-scale flume experiments on hydraulic roughness of submerged vegetation, *Tech. rep.*, HKV Consultants, Lelystad, Netherlands.

Naden, P., P. Rameshwaran, O. Mountford, and C. Robertson (2006), The influence of macrophyte growth, typical of eutropic conditions, on river flow velocities and turbulence production, *Hydrol. Processes*, *20*, 3915–3938.

Neary, V. S. (2003), Numerical solution of fully-developed flow with vegetative resistance, *J. Eng. Mech.*, *129*(5), 558–563.

Nepf, H. M. (1999), Drag, turbulence, and diffusion in flow trough emergent vegetation, *Water Resour. Res.*, *35*(2), 479–489.

Nezu, I., and K. Onitsuka (2001), Turbulent structures in partly vegetated open-channel flows with LDA and PIV measurements, *J. Hydraulic Res.*, *39*(6), 629–642.

Nikora, V., A. N. Sukhodolov, and P. M. Rowinski (1997), Statistical sand wave dynamics in one-directional water flows, *J. Fluid Mech.*, *351*, 17–39.

Nikuradse, J. (1933), Strömungsgesetze in rauhen Rohren, *Forschungsheft VDI Verlag Berlin*, *B*(362).

Petryk, S., and G. Bosmajian (1975), Analysis of flow trough vegetation, *J. Hydraulics Div.*, *101*(HY7), 871–884.

Poggi, D., A. Porporato, L. Ridolfi, J. D. Albertson, and G. G. Katul (2004), The effect of vegetation density on canopy sub-layer turbulence, *Boundary-Layer Meteorol.*, *111*, 565–587.

Pope, S. B. (2000), *Turbulent Flows*, third ed., Cambridge Univ. Press, New York.

Pouquet, A., U. Frisch, and J. P. Chollet (1983), Turbulence with a spectral gap, *Phys. Fluids*, *26*(4), 877–879.

Raupach, M. R. (1992), Drag and drag partition on rough surfaces, *Boundary-Layer Meteorol.*, *60*, 375–395.

Raupach, M. R., P. A. Coppin, and B. J. Legg (1986), Experiments on scalar dispersion within a model plant canopy: part 1. The turbulence structure, *Boundary-Layer Meteorol.*, *35*, 21–52.

Raupach, M. R., J. J. Finnigan, and Y. Brunet (1996), Coherent eddies and turbulence in vegetation canopies: The mixing-layer analogy, *Boundary-Layer Meteorol.*, *78*, 351–382.

Ree, W. O., and F. R. Crow (1977), Friction factors for vegetated waterways of small slope, *Tech. Rep. Publication S-151*, US Department of Agriculture, Agricultural Research Service.

Schlichting, H. (1979), *Boundary Layer Theory*, 7th ed., McGraw-Hill, New York.

Shimizu, Y., and T. Tsujimoto (1994), Numerical analysis of turbulent open-channel flow over vegetation layer using a $k - \varepsilon$ turbulence model, *J. Hydroscience Hydraulic Eng.*, *11*(2), 57–67.

Silberman, E., R. W. Carter, H. A. Einstein, J. Hinds, and R. W. Powell (1963), Friction factors in open channels: Progress report by the Task Force on Friction Factors in Open Channels of the Committee on Hydromechanics of the Hydraulics Division, *J. Hydraulics Div.*, *89*(HY2), 97–143.

Smart, G. M., M. J. Duncan, and J. M. Walsh (2002), Relatively rough flow resistance equations, *J. Hydraulic Eng.*, *128*(6), 568–578.

Stephan, U., and D. Gutknecht (2002), Hydraulic resistance of submerged flexible vegetation, *J. Hydrol.*, *269*, 27–43.

Stone, B. M., and H. T. Shen (2002), Hydraulic resistance of flow in channels with cylindrical roughness, *J. Hydraulic Eng.*, *128*(5), 500–506.

Strickler, A. (1923), Beitrage zur Frage der Geschwindigkeitsformel und der Rauhigkeitszahlen für Ströme, Kanäle und geschlossene Leitungen, *Mitteilungen des Amtes für Wasserwirtschaft 16*, Eidg. Department des Innern, Bern, Switserland.

Sumner, D., J. L. Heseltine, and O. J. P. Dansereau (2004), Wake structure of a finite circular cylinder of small aspect ratio, *Exp. Fluids*, *37*(5), 720–730.

van Velzen, E. H., P. Jesse, P. Cornelissen, and H. Coops (2003), Stromingsweerstand vegetatie in uiterwaarden, *Handboek report 2003.028*, RIZA, Arnhem, Netherlands.

Wilson, C. A. M. E., T. Stoesser, P. D. Bates, and A. Batemann-Pinzen (2003), Open channel flow through different forms of submerged flexible vegetation, *J. Hydraulic Eng.*, *129*, 847–853.

Wu, F.-C., H. W. Shen, and C. Y-J (1999), Variation of roughness coefficients for unsubmerged and submerged vegetation, *J. Hydraulic Eng.*, *125*(9), 934–942.

Yen, B. C. (2002), Open channel flow resistance, *J. Hydraulic Eng.*, *128*(1), 20–39.

D. C. M. Augustijn, S. J. M. H. Hulscher, and F. Huthoff, Faculty of Engineering Technology, Water Engineering and Management, University of Twente, P.O. Box 217, 7500 AE Enschede, Netherlands. (f.huthoff@utwente.nl)